

Kinetics Study of the Esterification Reaction of Diethylene Glycol Monobutyl Ether with Acetic Acid Catalyzed by Heteropolyanion-Based Ionic Liquids

Yong Liu,* Yitao Wang, Cuiping Zhai, Weiping Chen, and Congzhen Qiao*

Institute of Fine Chemistry and Engineering, College of Chemistry and Chemical Engineering, Henan University, Kaifeng 475004, China

S Supporting Information

ABSTRACT: Novel heteropolyanion-based ionic liquids (HPA-ILs) were obtained by combining Keggin heteropolyanions and organic cations and used as catalysts for an esterification reaction. The kinetic behaviors in the esterification of diethylene glycol monobutyl ether (DGBE) with acetic acid in the presence of HPA-ILs as catalysts were investigated systematically. Different types of HPA-ILs were used for the esterification of DGBE. Compared with H_2SO_4 , $\text{H}_3\text{PW}_{12}\text{O}_{40}$, and Amberlyst-15 resins, $[\text{BSEt}_3\text{N}]_3\text{PW}_{12}\text{O}_{40}$ and $[\text{BSmim}]_3\text{PW}_{12}\text{O}_{40}$ exhibited excellent catalytic activities. The influences of reaction temperature, catalyst dosage, and reactant molar ratio on the conversion of DGBE were studied in detail. The kinetic data were successfully correlated by a pseudohomogeneous (PH) model in the temperature range of 343.15–363.15 K. The simulation values obtained by the kinetic model were in good agreement with the experimental data. Moreover, $[\text{BSEt}_3\text{N}]_3\text{PW}_{12}\text{O}_{40}$ and $[\text{BSmim}]_3\text{PW}_{12}\text{O}_{40}$ could be easily recovered and reused six times without any obvious decrease in catalytic activity.

1. INTRODUCTION

Diethylene glycol butyl ether acetate (DGBA) is a colorless liquid with a mild, fruity, ether-like odor. It is widely used as a solvent for printing inks, resins, lacquers, and gums because of its high boiling point and multiple functional groups. DGBA is mainly produced by the esterification reaction of diethylene glycol monobutyl ether (DGBE) with acetic acid using mineral acids, such as H_2SO_4 , HCl , and H_3PO_4 , as catalysts. However, these acids always entail some drawbacks of low selectivity, equipment corrosion, environmental pollution, and tedious purification of the products.

To overcome these problems, some solid heterogeneous catalysts, such as zeolites,^{1,2} metal oxide,^{3,4} cation exchange resins,^{5–7} and heteropolyacids (HPAs),^{8–11} have been studied to replace mineral acid catalysts in many esterification reactions. In particular, HPAs with Keggin structures have attracted increasing attention because of their low toxicity, high acidity, and tunable redox properties. However, the low surface areas (<10 m²/g) and water solubilities of HPAs usually hinder their practical application.^{12,13} To overcome these disadvantages, immobilization of HPAs onto porous solid supports has been regarded as an effective method for enhancing their properties and obtaining better catalytic performance in a number of esterification reactions.^{14–17} Nevertheless, HPAs supported on carriers always suffer from high transfer resistance, slow reaction rates, and leaching of active sites owing to weak interactions between HPAs and most supports.^{18,19} Therefore, it is very necessary to develop highly active, environmentally friendly, and easily recyclable catalysts for the esterification of DGBE with acetic acid.

As clean catalysts and excellent solvents, ionic liquids (ILs) have gained extensive attention because of their unique physical and chemical properties, such as high thermal stability, negligible vapor pressure, remarkable solubility, and reus-

ability.^{20–22} Thus, esterification reactions catalyzed by ILs have gained increasing attention.^{23–25} Although these works showed high conversions and selectivities for the investigated esterification reactions, several disadvantages of ILs still limit their practical use, including high contents of ILs (20–300 mol %) needed in the reaction media, relatively long reaction times, and the need to remove byproduct from the IL phase in IL recycling experiments.^{26,27} In light of the advantages of ILs and HPAs, a novel type of HPA-based ionic hybrids combining Keggin heteropolyanions with IL cations has attracted intense interest. Leng et al.²⁷ first reported the application of heteropolyacid-based ionic liquids (HPA-ILs) in esterification reaction. These catalysts were applied as “reaction-induced self-separation catalysts” for esterification reactions with a poly-(carboxylic acid) or polyol. After the reaction, the catalysts could be easily recovered by simple filtration. To further extend the study of these HPA-ILs, several HPA-ILs have been synthesized and used as catalysts for transesterification, oxidation, and desulfurization reactions.^{26,28–32}

In addition, kinetic studies are very important for reaction engineering, but only a small number of researchers have carried out kinetic studies of reactions catalyzed by ILs. Tao and co-worker^{25,33} reported the kinetics of the esterification reaction of *n*-butanol with acetic acid and the ketalization reaction of cyclohexanone with glycol in the presence of Brønsted acidic ionic liquids as catalysts. Cui et al.³⁵ also reported the kinetics of the transesterifications of methyl acetate and *n*-butanol using ILs as catalysts. To the best of our knowledge, no kinetic studies of esterification reactions

Received: June 11, 2014

Revised: August 14, 2014

Accepted: September 2, 2014

Published: September 2, 2014

catalyzed by HPA-ILs have been reported so far. Therefore, it is necessary to study the kinetics of esterification reactions of DGBE with acetic acid using HPA-ILs as catalysts. The information on kinetics can provide optimal operating parameters for the production of DGBA.

Therefore, in this work, several Keggin tungstophosphoric acid-based ILs were prepared. The kinetics of the esterification reactions of acetic acid with DGBE using HPA-ILs as catalysts were also studied. The influences of various parameters such as the type of HPA-IL, reaction temperature, catalyst dosage, and initial reactant molar ratio were studied in detail. A pseudohomogeneous (PH) kinetic model was proposed to correlate the experimental data, and corresponding kinetic parameters were estimated.

2. EXPERIMENTAL SECTION

2.1. Materials. Phosphotungstic acid ($\text{H}_3\text{PW}_{12}\text{O}_{40}$) and *n*-butyl bromide ($\text{C}_4\text{H}_9\text{Br}$) were purchased from Sinopharm Chemical Reagent, Shanghai, China. Amberlyst-15 resin in H^+ form was purchased from Rohm and Haas Company. 1,4-Butyl sultone (purity $\geq 99\%$) and 1-methylimidazole (purity $\geq 99\%$) were obtained from Aladdin Reagent Co., Ltd., Shanghai, China. Other reagents such as triethylamine, acetic acid, sulfuric acid, and diethylene glycol monobutyl ether were of analytical grade and were used without any further purification unless otherwise stated.

2.2. Preparation and Characterization of HPA-ILs.

Several HPA-ILs composed of different cations and the $\text{PW}_{12}\text{O}_{40}^{3-}$ anion were synthesized in this work (Figure 1).

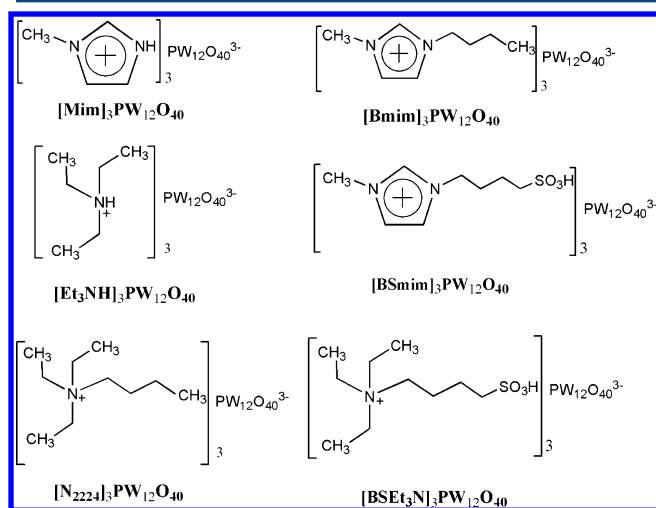


Figure 1. Structures of six HPA-ILs.

These HPA-ILs were characterized by ^1H nuclear magnetic resonance (NMR) (Bruker DPX-400) and Fourier transform infrared (FT-IR) spectroscopies and thermogravimetric analysis–differential scanning calorimetry (TGA–DSC). The results of characterization can be found in the Supporting Information. Elemental analyses (C, H, N) for six types of HPA-ILs were carried out on a CHN elemental analyzer (vario EL, Elementar Analysensysteme GmbH, Hanau, Germany). The elemental analysis results are summarized in Table S1 of the Supporting Information. As can be seen in Table S1 (Supporting Information), the measured C, N, and H weight percentages were in good agreement with the calculated values. Moreover, the pH values of the HPA-IL solutions (0.01 mol

L^{-1}) were measured with a PHS-3C pH meter equipped with a recorder obtained from Shanghai Leici Instrument Inc., Shanghai, China. The experimental results are summarized in Table 1.

Table 1. Comparison of the Conversions of DGBE and pH Values of the DMSO Solution Using Different Catalysts

entry	catalyst	pH ^a	time (h)	conversion of DGBE ^b (%)
1	[BSmim] ₃ PW ₁₂ O ₄₀	2.58	1	62.8
			4	76.2
2	[BSEt ₃ N] ₃ PW ₁₂ O ₄₀	2.28	1	66.5
			4	80.4
3	[Mim] ₃ PW ₁₂ O ₄₀	5.85	1	2.1
			4	8.0
4	[Et ₃ NH] ₃ PW ₁₂ O ₄₀	6.04	1	1.7
			4	7.4
5	[Bmim] ₃ PW ₁₂ O ₄₀	5.90	1	1.9
			4	7.6
6	[N ₂₂₂₄] ₃ PW ₁₂ O ₄₀	6.10	1	1.8
			4	6.2
7	H ₂ SO ₄	2.36	1	73.1
			4	80.5
8	H ₃ PW ₁₂ O ₄₀	2.20	1	74.5
			4	81.1
9	Amberlyst-15	–	1	56.6
			4	68.8

^aSolution in DMSO at 25 °C. ^bReaction conditions: temperature of 363.15 K, catalyst dosage of 5.0 wt % (based on the mass of all reactants), and acetic acid-to-DGBE molar ratio of 1:1. No byproducts were found by GC.

The procedure used for the synthesis of 1-(4-sulfonic acid)butyl-3-methylimidazolium phosphotungstate ([BSmim]₃PW₁₂O₄₀) was as follows: 1-Methylimidazole (0.1 mol) and 1,4-butane sultone (0.1 mol) were charged into a round-bottom flask (100 mL). Then, the mixture was agitated for 12 h at 80 °C. A white solid zwitterion formed, and the unreacted components were removed by repeated washing with ether (2 × 5 mL). The white solid was dried under a vacuum (<10 mmHg). Then, a stoichiometric amount of an aqueous solution of H₃PW₁₂O₄₀ was added, and the mixture was agitated for 24 h at room temperature. Water was removed under a vacuum to give the product as a solid. The synthesis of *N*-(4-sulfonic acid)butyl triethylammonium phosphotungstate ([BSEt₃N]₃PW₁₂O₄₀) was also performed according to the process described for [BSmim]₃PW₁₂O₄₀.

The synthesis of 1-methylimidazole phosphotungstate ([Mim]₃PW₁₂O₄₀) was performed as follows: 1-Methylimidazole (0.3 mol) was charged into a round-bottom flask. H₃PW₁₂O₄₀ (0.1 mol) aqueous solution was added slowly to the 1-methylimidazole solution at room temperature under stirring, and then the mixture was agitated for 24 h. The mixture was filtered, washed, and dried under a vacuum to give the product as a white solid. The preparation process of *N*-triethylammonium phosphotungstate ([Et₃NH]₃PW₁₂O₄₀) was similar to the process used for [Mim]₃PW₁₂O₄₀.

1-Butyl-3-methylimidazolium phosphotungstate ([Bmim]₃PW₁₂O₄₀) was prepared as follows: First, 1-butyl-3-methylimidazolium bromide ([Bmim][Br]) was prepared by placing 0.1 mol of 1-methylimidazole, 0.1 mol of 1-bromobutane, and 50 mL of ethanol into a round-bottom flask (100 mL). Then, the mixture was stirred vigorously for 24

h at 80 °C. The unreacted components and solvent were removed by rotary evaporation, and [Bmim][Br] was dried in a vacuum at 60 °C for 12 h. Then, 3 times the stoichiometric amount of [Bmim][Br] was added to an aqueous solution of $\text{H}_3\text{PW}_{12}\text{O}_{40}$. The mixture was agitated at room temperature for 24 h, and a white solid formed. The precipitate was filtered and washed with ultrapure water several times. This process was monitored by aqueous AgNO_3 until the filtrate no longer contained AgBr ; the precipitate was then dried under a vacuum. The synthesis of butyltriethylammonium phosphotungstate ($[\text{N}_{2224}]_3\text{PW}_{12}\text{O}_{40}$) was performed according to the process described for $[\text{Bmim}]_3\text{PW}_{12}\text{O}_{40}$ using triethylamine and 1-bromobutane.

2.3. Apparatus and Procedure. The kinetics of the esterification reactions were studied in a glass stirred-tank reactor (50 mL) placed in a constant-temperature water bath to hold the set temperature. In a typical run, 0.01 mol of acetic acid and 0.01 mol of DGBE were placed into the reactor, which was equipped with a reflux condenser. After the reaction temperature increased to the set value, the HPA-IL catalyst was added to the reactor, and the mixture was then allowed to react for 4 h with vigorous stirring. The time corresponding to the addition of the catalyst was considered as the zero reaction time for the run. During each experiment, samples were removed from the reactor at specific time intervals, cooled rapidly to about 273.15 K in an ice bath to avoid any further reaction, and then analyzed by gas chromatography (GC).

2.4. Analysis. The reaction mixtures were analyzed on a gas chromatograph (Shimadzu GC-17A) equipped with a DB-1 capillary column (30 m \times 0.539 mm \times 1.50 μm) and a hydrogen flame ionization detector (FID) with nitrogen as the carrier gas. The temperatures of the inlet and detector were set at 563.15 and 573.15 K, respectively.

3. RESULTS AND DISCUSSION

3.1. Catalyst Performance. The esterification reactions of acetic acid with DGBE using different HPA-ILs and other acid catalysts were carried out to test their catalytic activities under the same conditions. The results are reported in Table 1 and Figure 2. As can be seen in Table 1, the six HPA-IL catalysts tested exhibited different catalytic activities. There was a close

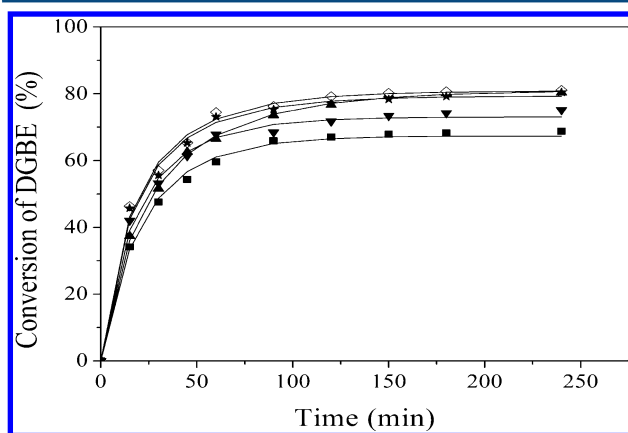


Figure 2. Conversions of DGBE obtained using (▼) $[\text{Bmim}]_3\text{PW}_{12}\text{O}_{40}$, (▲) $[\text{BSEt}_3\text{N}]_3\text{PW}_{12}\text{O}_{40}$, (◇) $\text{H}_3\text{PW}_{12}\text{O}_{40}$, (★) H_2SO_4 , and (■) Amberlyst-15 resins as catalysts. Reaction conditions: temperature of 363.15 K, catalyst dosage of 5.0 wt % (based on the mass of all reactants), and acetic acid-to-DGBE molar ratio of 1:1.

relationship between the catalytic performances of the HPA-ILs and their acidities. Among the HPA-ILs, $[\text{BSEt}_3\text{N}]_3\text{PW}_{12}\text{O}_{40}$ and $[\text{BSmim}]_3\text{PW}_{12}\text{O}_{40}$ with butyl sulfonic acid showed much higher catalytic performances than $[\text{N}_{2224}]_3\text{PW}_{12}\text{O}_{40}$ and $[\text{Bmim}]_3\text{PW}_{12}\text{O}_{40}$ under the same conditions, because of their strong acidities. The conversion of DGBE reached 80.4% and 76.2% at 4 h using $[\text{BSmim}]_3\text{PW}_{12}\text{O}_{40}$ and $[\text{BSEt}_3\text{N}]_3\text{PW}_{12}\text{O}_{40}$, respectively, as catalysts. In comparison, in the presence of $[\text{Et}_3\text{NH}]_3\text{PW}_{12}\text{O}_{40}$ and $[\text{Mim}]_3\text{PW}_{12}\text{O}_{40}$, the conversions of DGBE at 4 h were only 7.4% and 8.0%, respectively. Therefore, these results indicate that the different cationic structures of HPA-ILs can affect their acidities conveniently and that the catalytic activity becomes better if the acidity of the HPA-IL is stronger.

For comparison, the esterification reaction was also investigated in the presence of H_2SO_4 , $\text{H}_3\text{PW}_{12}\text{O}_{40}$, and the strong acidic cation-exchange resin Amberlyst-15. As can be seen in Table 1 and Figure 2, in contrast to the other catalysts, $\text{H}_3\text{PW}_{12}\text{O}_{40}$ showed the best catalytic performance. However, $\text{H}_3\text{PW}_{12}\text{O}_{40}$ has good solubility, which makes its isolation from the reaction mixture difficult. In addition, it was found that the conversion of DGBE at 4 h using Amberlyst-15 resin as the catalyst was lower than those obtained using $[\text{BSEt}_3\text{N}]_3\text{PW}_{12}\text{O}_{40}$ and $[\text{BSmim}]_3\text{PW}_{12}\text{O}_{40}$ as catalysts. It is possible that Amberlyst-15 resin, as a heterogeneous catalyst, has a high mass-transfer resistance, leading to a relatively lower catalytic activity.³³ Moreover, as heterogeneous catalysts, $[\text{BSEt}_3\text{N}]_3\text{PW}_{12}\text{O}_{40}$ and $[\text{BSmim}]_3\text{PW}_{12}\text{O}_{40}$ can be easily separated from the reactants by simple filtration. Thus, $[\text{BSmim}]_3\text{PW}_{12}\text{O}_{40}$ and $[\text{BSEt}_3\text{N}]_3\text{PW}_{12}\text{O}_{40}$ were found to have promising application prospects in the production of DGBA and were thus used for further kinetics experiments.

3.2. Effect of Temperature. The influence of the reaction temperature in the range of 343.15–363.15 K on the conversion of DGBE was studied using $[\text{BSmim}]_3\text{PW}_{12}\text{O}_{40}$ and $[\text{BSEt}_3\text{N}]_3\text{PW}_{12}\text{O}_{40}$ as catalysts under the same reaction conditions. As shown in Figure 3, the conversion of DGBE increased with increasing reaction temperature. For $[\text{BSEt}_3\text{N}]_3\text{PW}_{12}\text{O}_{40}$, the conversion of DGBE at 4 h increased obviously from 58% to 80% when the reaction temperature was increased from 343.15 to 363.15 K, indicating that an increase in reaction temperature is beneficial in enhancing the conversion of DGBE. This is because an increase in temperature brings about more successful collisions between reactants that have sufficient activation energy to break the bonds and form products and thus lead to a higher conversion of DGBE. A similar phenomenon was also observed in the presence of $[\text{BSmim}]_3\text{PW}_{12}\text{O}_{40}$ as the catalyst in the esterification reaction.

3.3. Effect of Catalyst Dosage. The influence of catalyst dosage on the conversion of DGBE was studied using $[\text{BSmim}]_3\text{PW}_{12}\text{O}_{40}$ and $[\text{BSEt}_3\text{N}]_3\text{PW}_{12}\text{O}_{40}$ as catalysts. As can be seen in Figure 4, the conversion of DGBE increased with increasing catalyst dosage. When the catalyst dosage of $[\text{BSEt}_3\text{N}]_3\text{PW}_{12}\text{O}_{40}$ was increased from 1.0 to 3.0 wt %, the conversion of DGBE at 4 h increased obviously from 58% to 75%. This is because a higher catalyst dosage provides more available active sites for the esterification reaction, which leads to a higher conversion of DGBE. However, when the amount of $[\text{BSEt}_3\text{N}]_3\text{PW}_{12}\text{O}_{40}$ was further increased to 5.0 wt %, only a slight increase in the conversion of DGBE was observed, suggesting that the further increase in the amount of catalyst was not very necessary for the conversion of the reactants.

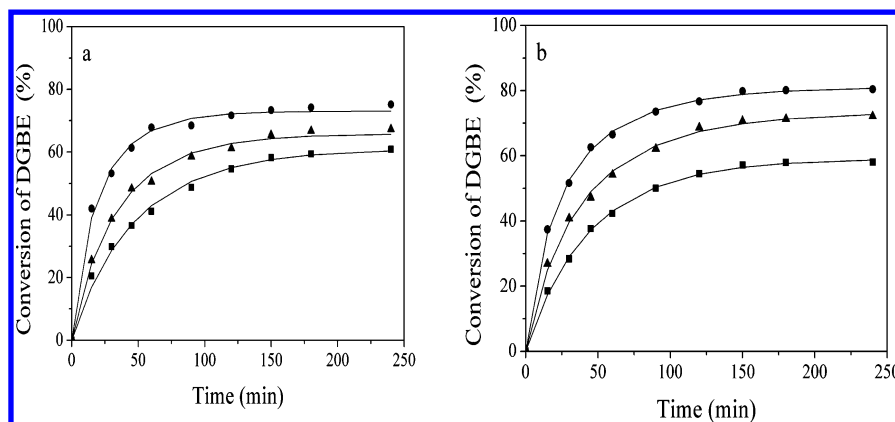


Figure 3. Effects of temperature on the conversion of DGBE in the presence of (a) $[\text{BSmim}]_3\text{PW}_{12}\text{O}_{40}$ and (b) $[\text{BSEt}_3\text{N}]_3\text{PW}_{12}\text{O}_{40}$ as catalysts at temperatures of (■) 343.15, (▲) 353.15, and (●) 363.15 K with an acetic acid-to-DGBE molar ratio of 1:1 and a catalyst dosage of 5.0 wt % (based on the mass of all reactants).

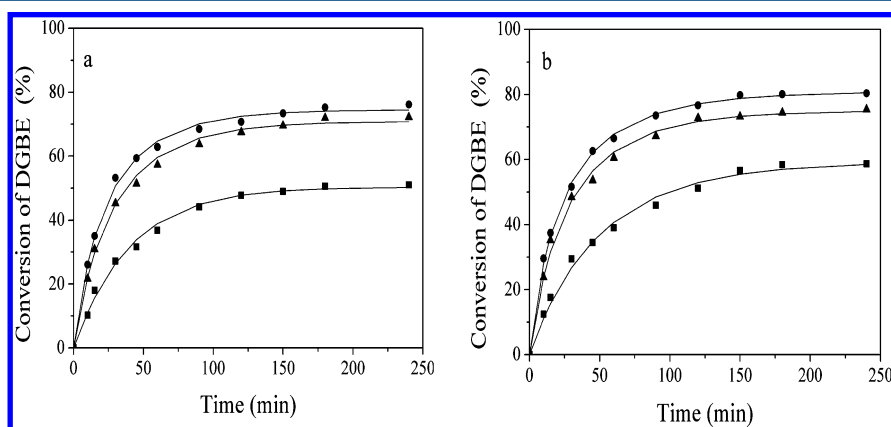


Figure 4. Effects of catalyst dosage on the conversion of DGBE using (a) $[\text{BSmim}]_3\text{PW}_{12}\text{O}_{40}$ and (b) $[\text{BSEt}_3\text{N}]_3\text{PW}_{12}\text{O}_{40}$ as catalysts at 363.15 K with an acetic acid-to-DGBE molar ratio of 1:1 and catalyst dosages of (■) 1.0, (▲) 3.0, and (●) 5.0 wt % (based on the mass of all reactants).

Because the reaction rate was found to be related to the catalyst loading, the relationship between the initial reaction rate (r_0) and the catalyst dosage was studied. As shown in Figure 5, the initial reaction rate increased with increasing catalyst dosage, which might be because the number of available active sites is proportional to the catalyst dosage for the esterification reaction of DGBE with acetic acid. The initial reaction rate is a function of catalyst dosage and can be expressed as

$$-r_0 = EC_{\text{cat}} + F \quad (1)$$

where C_{cat} is the catalyst loading (kg L^{-1}) and E and F are constants. This equation is valid only at 363.15 K and the acetic acid-to-DGBE molar ratio of 1:1 used for the experiments. From Figure 5, the values of E and F were determined to be 0.361 and 0.00962, respectively, for $[\text{BSmim}]_3\text{PW}_{12}\text{O}_{40}$ and 0.435 and 0.00935, respectively, for $[\text{BSEt}_3\text{N}]_3\text{PW}_{12}\text{O}_{40}$.

3.4. Effect of Initial Reactant Molar Ratio. The effect of different initial acetic acid-to-DGBE molar ratio was also investigated using $[\text{BSEt}_3\text{N}]_3\text{PW}_{12}\text{O}_{40}$ as the catalyst. As can be seen in Figure 6, the conversion of DGBE was influenced by the initial molar ratio of the reactants. The conversion of DGBE at 4 h increased markedly from 47% to 87% as the initial acetic acid-to-DGBE molar ratio was increased from 1:2 to 1.5:1. This result can be attributed to the fact that increasing the concentration of the reactant acetic acid helps shift the reaction equilibrium toward the product side because the esterification reaction of DGBE with acetic acid is a reversible reaction. However, when the relative amount of acetic acid was further increased to 2:1, the conversion of DGBE exhibited no marked increase. This might be because the reactant DGBE was diluted by increasing the amount of acetic acid, which prevented DGBE from adsorbing on the catalyst acid sites. This implies that excess acetic acid is not beneficial for the esterification of DGBE.

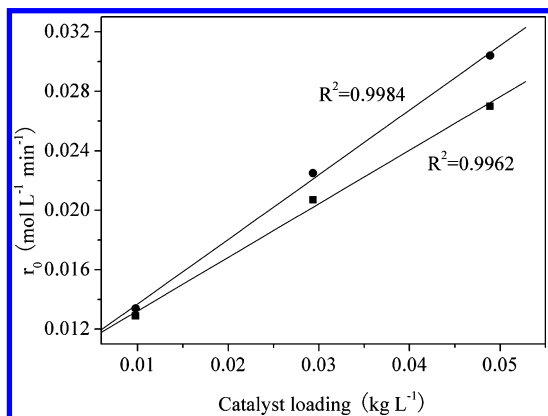


Figure 5. Effects of catalyst dosage on the initial reaction rate using (■) $[\text{BSmim}]_3\text{PW}_{12}\text{O}_{40}$ and (●) $[\text{BSEt}_3\text{N}]_3\text{PW}_{12}\text{O}_{40}$ as catalysts at 363.15 K with an acetic acid-to-DGBE molar ratio of 1:1.

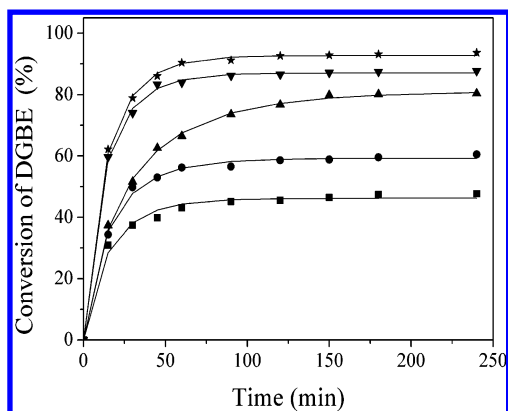


Figure 6. Effects of the initial reactant molar ratio on the conversion of DGBE using $[\text{BSEt}_3\text{N}]_3\text{PW}_{12}\text{O}_{40}$ as the catalyst at 363.15 K with acetic acid-to-DGBE molar ratios of (■) 1:2, (●) 1:1.5, (▲) 1:1, (▼) 1.5:1, and (★) 2:1 and a catalyst dosage of 5.0 wt % (based on the mass of all reactants).

3.5. Chemical Equilibrium. Kinetic experiments were conducted at different temperatures to obtain the chemical equilibrium constants under the same conditions. Samples were withdrawn from the reactor after specific time intervals and were analyzed until chemical equilibrium was reached. The chemical equilibrium constant was obtained from the equilibrium concentration according to the equation

$$K_e = \frac{C_{\text{DBAC}}C_{\text{H}_2\text{O}}}{C_{\text{DGBE}}C_{\text{acid}}} \quad (2)$$

where K_e is the equilibrium constant and C_i is the equilibrium concentration of component i (mol L^{-1}).

The dependency of the equilibrium constant K_e on the temperature can be found from a plot of $\ln K_e$ versus the reciprocal temperature ($1/T$), as given in Figure 7. It was found

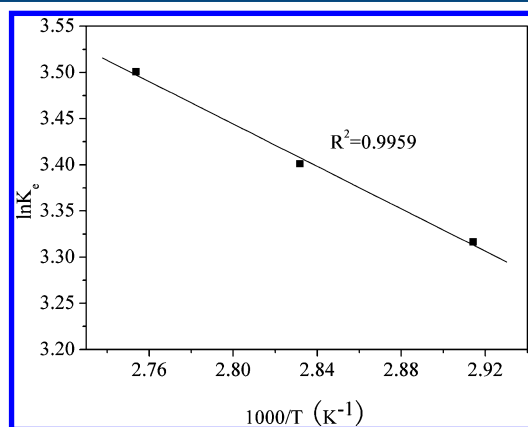


Figure 7. Effects of reaction temperature on the chemical equilibrium constant.

that the equilibrium constant increased with increasing temperature, which indicates the esterification reaction of DGBE with acetic acid is an endothermic reaction. The equilibrium constant can be expressed as

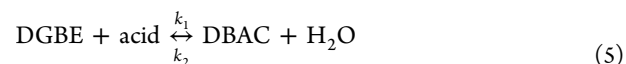
$$\ln K_e = 6.66 - \frac{1147.1}{T} \quad (3)$$

The reaction enthalpy ($\Delta_r H^0$) and entropy ($\Delta_r S^0$) were estimated using the van't Hoff equation^{33,34}

$$\ln K_e = \frac{-\Delta_r H^0}{RT} + \frac{\Delta_r S^0}{R} \quad (4)$$

The reaction enthalpy $\Delta_r H^0$ and entropy $\Delta_r S^0$ were found to be 0.96 kJ mol^{-1} and $55.37 \text{ J mol}^{-1} \text{ K}^{-1}$, respectively. The positive reaction enthalpy again indicates that the esterification reaction of DGBE with acetic acid is endothermic.

3.6. Reaction Kinetic Modeling. The esterification reaction equation of acetic acid with DGBE can be written as



A pseudohomogeneous (PH) model can be used for systems in which one of the reactants or solvents is highly polar. Many esterification reactions can be expressed using a PH model.^{5-7,34} In this work, the kinetic equations for the esterification of acetic acid with DGBE using $[\text{BSEt}_3\text{N}]_3\text{PW}_{12}\text{O}_{40}$ and $[\text{BSmim}]_3\text{PW}_{12}\text{O}_{40}$ as catalysts were established according to the PH model. The esterification reaction is known to be reversible second-order reactions. Therefore, the PH model can be written as

$$\begin{aligned} r &= M_{\text{cat}}(k_1 C_{\text{DGBE}} C_{\text{acid}} - k_2 C_{\text{DBAC}} C_{\text{H}_2\text{O}}) \\ &= M_{\text{cat}} k_1 \left(C_{\text{DGBE}} C_{\text{acid}} - \frac{1}{K_e} C_{\text{DBAC}} C_{\text{H}_2\text{O}} \right) \end{aligned} \quad (6)$$

where $K_e = k_1/k_2$ is the equilibrium constant. M_{cat} is the catalyst dosage per unit volume; C_i is the molar concentration of component i ; and k_1 and k_2 are the rate constants of the forward and reverse reactions, respectively.

A fourth-order Runge–Kutta method was used to numerically integrate the kinetic equations. The kinetic parameters were estimated by minimizing the sum of residual squares (SRS) between the values for the conversion of DGBE calculated according to the PH model and obtained by experiments

$$\text{SRS} = \sum_{\text{samples}} (x_{\text{exp}} - x_{\text{calc}})^2 \quad (7)$$

where SRS is the minimum sum of residual squares and x is the conversion of DGBE. The subscripts exp and calc represent experimental and calculated values, respectively.

The simulated values obtained by the PH model were compared to the experimental values at different reaction temperatures, catalyst dosages, and initial reactant molar ratios. The results are shown in Figures 3, 4, and 6, respectively. It can be seen that the conversions of DGBE calculated by the reaction kinetic model were in good agreement with those obtained from experiments. This indicates that the PH model provides a good description of the kinetic behavior for the esterification of DGBE with acetic acid using $[\text{BSEt}_3\text{N}]_3\text{PW}_{12}\text{O}_{40}$ and $[\text{BSmim}]_3\text{PW}_{12}\text{O}_{40}$ as catalysts.

The dependence of the rate constants on temperature can be expressed by the Arrhenius law

$$\ln k = \ln k_0 - \frac{E_a}{RT} \quad (8)$$

The activation energy (E_a) and pre-exponential factor (k_0) were obtained from eq 8 by plotting $\ln k$ versus $1/T$. The slope of straight lines ($-E_a/R$) and the intercept on the ordinate ($\ln k_0$) are shown in Figure 8. The values of the pre-exponential factors ($k_{0,1}$, $k_{0,2}$) and activation energies ($E_{a,1}$, $E_{a,2}$) are reported in

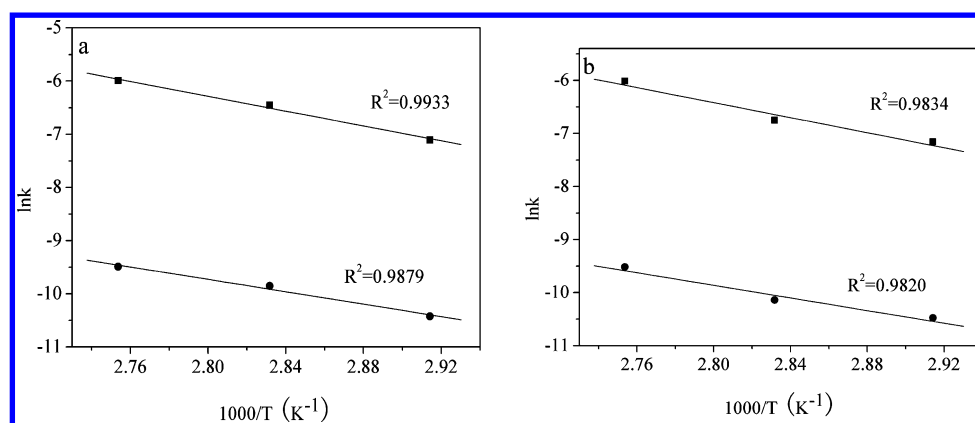


Figure 8. Arrhenius plots for the esterification of DGBE with acetic acid using (a) $[\text{BSEt}_3\text{N}]_3\text{PW}_{12}\text{O}_{40}$ and (b) $[\text{BSmim}]_3\text{PW}_{12}\text{O}_{40}$ as catalysts: (■) k_1 of the forward reaction and (●) k_2 of the reverse reaction.

Table 2. It was found that the activation energies and pre-exponential factors for $[\text{BSEt}_3\text{N}]_3\text{PW}_{12}\text{O}_{40}$ and

Table 2. Parameters of the PH Model

catalyst	$k_{0,i}$ (mol min ⁻¹)		$E_{a,i}$ (kJ mol ⁻¹)	
	$i = 1$	$i = 2$	$i = 1$	$i = 2$
$[\text{BSEt}_3\text{N}]_3\text{PW}_{12}\text{O}_{40}$	5.60×10^5	7.21×10^2	57.97	48.83
$[\text{BSmim}]_3\text{PW}_{12}\text{O}_{40}$	6.85×10^5	8.81×10^2	58.96	49.42

$[\text{BSmim}]_3\text{PW}_{12}\text{O}_{40}$ catalytic systems were similar to each other. At the same time, our kinetic study indicated that $[\text{BSEt}_3\text{N}]_3\text{PW}_{12}\text{O}_{40}$ and $[\text{BSmim}]_3\text{PW}_{12}\text{O}_{40}$ have similar catalytic activities. Therefore, the obtained kinetic information has promising prospects in designing the esterification reaction of DGBE with acetic acid and optimizing various operating parameters.

3.7. Recycling of Catalyst. The stability and reusability of catalysts are important factors for their potential application in industry. Thus, the reusability characteristics of $[\text{BSEt}_3\text{N}]_3\text{PW}_{12}\text{O}_{40}$ and $[\text{BSmim}]_3\text{PW}_{12}\text{O}_{40}$ in the esterification reaction of DGBE with acetic acid were investigated. Because the esterification reactions of DGBE with acetic acid catalyzed by $[\text{BSEt}_3\text{N}]_3\text{PW}_{12}\text{O}_{40}$ and $[\text{BSmim}]_3\text{PW}_{12}\text{O}_{40}$ are liquid–solid biphasic heterogeneous reactions, the solid catalyst could be easily recovered by filtration, washed with acetone three times, and dried under a vacuum at 60 °C for 12 h. The recovered catalyst was then used in the next run. As shown in Figure 9, the conversions of DGBE in six consecutive runs exhibited no significant decrease in activity, which indicates that $[\text{BSEt}_3\text{N}]_3\text{PW}_{12}\text{O}_{40}$ and $[\text{BSmim}]_3\text{PW}_{12}\text{O}_{40}$ are sufficiently stable for the esterification reaction. The slight decrease in activity might be due to the slight loss of catalyst in the operation for recovering the catalyst.

4. CONCLUSIONS

The kinetics of the esterification reaction of DGBE with acetic acid using HPA-ILs as catalysts has been investigated. Compared with other HPA-ILs, H_2SO_4 , $\text{H}_3\text{PW}_{12}\text{O}_{40}$, and Amberlyst-15 resin, $[\text{BSEt}_3\text{N}]_3\text{PW}_{12}\text{O}_{40}$ and $[\text{BSmim}]_3\text{PW}_{12}\text{O}_{40}$ were found to have excellent catalytic activities. The experimental data were successfully correlated by a pseudohomogeneous (PH) model. The calculated results obtained using the estimated parameters were in good agreement with the experimental data. Activation energies of

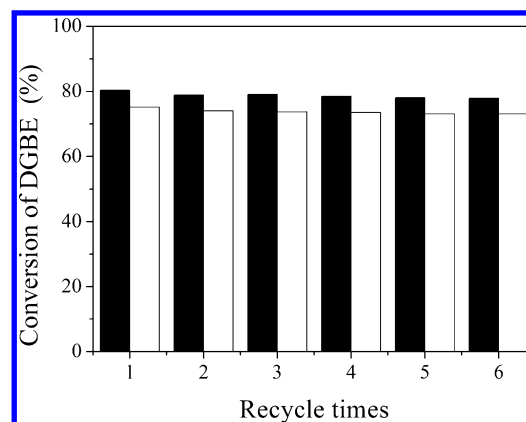


Figure 9. Reusability characteristics of (black) $[\text{BSEt}_3\text{N}]_3\text{PW}_{12}\text{O}_{40}$ and (white) $[\text{BSmim}]_3\text{PW}_{12}\text{O}_{40}$ catalysts at 363.15 K with an acetic acid-to-DGBE molar ratio of 1:1, a catalyst dosage of 5.0 wt % (based on the mass of all reactants), and a reaction time of 4 h.

57.97 and 58.96 kJ mol⁻¹ were obtained by the Arrhenius equation for $[\text{BSEt}_3\text{N}]_3\text{PW}_{12}\text{O}_{40}$ and $[\text{BSmim}]_3\text{PW}_{12}\text{O}_{40}$, respectively. Moreover, $[\text{BSEt}_3\text{N}]_3\text{PW}_{12}\text{O}_{40}$ and $[\text{BSmim}]_3\text{PW}_{12}\text{O}_{40}$ could be easily recovered and reused six times without any obvious decrease in catalytic activity, showing promising potential for application in industry.

■ ASSOCIATED CONTENT

📄 Supporting Information

Characterization of each HPA-IL, including ¹H NMR and FT-IR spectra; TGA–DSC curves; and C, H, N elemental analyses. This material is available free of charge via the Internet at <http://pubs.acs.org/>.

■ AUTHOR INFORMATION

Corresponding Authors

*E-mail: liuyong79@126.com (Y.L.).

*E-mail: qiaocongzheng@henu.edu.cn (C.Q.).

Notes

The authors declare no competing financial interest.

■ ACKNOWLEDGMENTS

This work was supported by the National Natural Science Foundation of China (No. 21206031) and the Foundation of Education Department of Henan Province of China (No. 13A150091).

■ ABBREVIATIONS

- [Bmim]Br = 1-butyl-3-methylimidazolium bromide
 [Bmim]₃PW₁₂O₄₀ = 1-butyl-3-methylimidazolium phosphotungstate
 [BSEt₃NH]₃PW₁₂O₄₀ = N-(4-sulfonic acid)butyl triethylammonium phosphotungstate
 [BSmim]₃PW₁₂O₄₀ = 1-(4-sulfonic acid)butyl-3-methylimidazolium phosphotungstate
 DGBA = diethylene glycol butyl ether acetate
 DGBE = diethylene glycol monobutyl ether
 [Et₃NH]₃PW₁₂O₄₀ = N-triethylammonium phosphotungstate
 HPA = heteropoly acids
 HPA-IL = heteropolyanion-based ionic liquid
 IL = ionic liquid
 [Mim]₃PW₁₂O₄₀ = 1-methylimidazole phosphotungstate
 [N₂₂₂₄]₃PW₁₂O₄₀ = butyltriethylammonium phosphotungstate
 PH = pseudohomogeneous
 SRS = minimum sum of residual squares

Nomenclature

- C = concentration, mol L⁻¹
 C_{cat} = catalyst dosage, kg L⁻¹
 E = constant
 E_{a,1} = activation energy of the forward reaction, kJ mol⁻¹
 E_{a,2} = activation energy of the reverse reaction, kJ mol⁻¹
 F = constant
 k = reaction rate constant, mol⁻¹ min⁻¹
 k₀ = pre-exponential factor, mol⁻¹ min⁻¹
 k₁ = forward reaction rate constant, mol⁻¹ min⁻¹
 k₂ = reverse reaction rate constant, mol⁻¹ min⁻¹
 K_c = equilibrium constant of the reaction
 M_{cat} = catalyst dosage per unit volume, g L⁻¹
 T = temperature, K
 x_{cal} = calculated conversion
 x_{exp} = experimental conversion
 Δ_rH⁰ = the reaction enthalpy, kJ mol⁻¹
 Δ_rS = entropy, J mol⁻¹ K⁻¹

■ REFERENCES

- Shekara, B. M. C.; Reddy, C. R.; Madhuranthakam, C. R.; Prakash, B. S. J.; Bhat, Y. S. Kinetics of esterification of phenylacetic acid with *p*-cresol over H-β zeolite catalyst under microwave irradiation. *Ind. Eng. Chem. Res.* **2011**, *50*, 3829–3835.
- Bedard, J.; Chiang, H.; Bhan, A. Kinetics and mechanism of acetic acid esterification with ethanol on zeolites. *J. Catal.* **2012**, *290*, 210–219.
- Mello, V. M.; Pousa, G. P. A. G.; Pereira, M. S. C.; Dias, I. M.; Suarez, P. A. Z. Metal oxides as heterogeneous catalysts for esterification of fatty acids obtained from soybean oil. *Fuel Process. Technol.* **2011**, *1*, 53–57.
- Li, K. T.; Wang, C. K. Esterification of lactic acid over TiO₂–Al₂O₃ catalysts. *Appl. Catal. A: Gen.* **2012**, *433*, 275–279.
- Jignesh, G.; Surendra, M.; Sanjay, M. Esterification of acetic acid with butanol in the presence of ion-exchange resins as catalysts. *Ind. Eng. Chem. Res.* **2003**, *42*, 2146–2155.
- Bastian, S.; Michael, D.; Julrgen, G. Esterification of ethylene glycol with acetic acid catalyzed by Amberlyst 36. *Ind. Eng. Chem. Res.* **2008**, *47*, 698–703.
- Tsai, Y. T.; Lee, M. J. Kinetics of catalytic esterification of propionic acid with methanol over Amberlyst 36. *Ind. Eng. Chem. Res.* **2011**, *50*, 1171–1176.
- Kozhevnikov, I. V. Catalysis by heteropoly acids and multi-component and multicomponent polyoxometalates in liquid-phase reactions. *Chem. Rev.* **1998**, *98*, 171–198.
- Cayo, E. G.; Letícia, O. L.; Abiney, L. C.; Márcio, J. S. Bioadditive synthesis from H₃PW₁₂O₄₀-catalyzed glycerol esterification with HOAc under mild reaction conditions. *Fuel Process. Technol.* **2012**, *102*, 46–52.
- Valeria, P.; Diego, M. R.; Juan, C. A.; Patricia, G. V.; Gustavo, P. R. Simple halogen-free synthesis of aryl cinnamates using Mo-Keggin heteropoly acids as catalyst. *Pure Appl. Chem.* **2012**, *84*, 529–540.
- Sergio, A. F.; Abiney, L. C.; Márcio, J. S. A novel kinetic study of H₃PW₁₂O₄₀-catalyzed oleic acid esterification with methanol via 1H NMR spectroscopy. *Fuel Process. Technol.* **2012**, *96*, 98–103.
- Sawant, D. P.; Vinu, A.; Justus, J.; Srinivasu, P.; Halligudi, S. B. Catalytic performances of silicotungstic acid/zirconia supported SBA-15 in an esterification of benzyl alcohol with acetic acid. *J. Mol. Catal. A: Chem.* **2007**, *276*, 150–157.
- Hafizi, A.; Ahmadpour, A.; Koolivand-Salooki, M.; Heravi, M. M.; Bamoharram, F. F. Comparison of RSM and ANN for the investigation of linear alkylbenzene synthesis over H₁₄[NaP₅W₃₀O₁₁₀]/SiO₂ catalyst. *J. Ind. Eng. Chem.* **2013**, *19*, 1981–1989.
- Kim, H. J.; Shul, Y. G.; Han, H. Synthesis of heteropolyacid (H₃PW₁₂O₄₀)/SiO₂ nanoparticles and their catalytic properties. *Appl. Catal. A* **2006**, *299*, 46–51.
- Abd, E.; Rahman, S.; Khder, H. M. A.; Hassan, M.; Samy, E. Acid catalyzed organic transformations by heteropoly tungstophosphoric acid supported on MCM-41. *Appl. Catal. A: Gen.* **2012**, *411*–412, 77–86.
- Ezzat, R.; Sara, E. Controlled immobilization of Keggin-type heteropoly acids on the surface of silica encapsulated γ-Fe₂O₃ nanoparticles and investigation of catalytic activity in the oxidative esterification of arylaldehydes with methanol. *J. Mol. Catal. A: Chem.* **2013**, *373*, 30–37.
- Varsha, B.; Anjali, P. Synthesis and characterization of 12-tungstosilicic acid anchored to MCM-41 as well as its use as environmentally benign catalyst for synthesis of succinate and malonate diesters. *Ind. Eng. Chem. Res.* **2011**, *50*, 13693–13702.
- Liu, Y.; Murata, K.; Inaba, M. Direct oxidation of benzene to phenol by molecular oxygen over catalytic systems containing Pd(OAc)₂ and heteropolyacid immobilized on HMS or PIM. *J. Mol. Catal. A: Chem.* **2006**, *256*, 247–255.
- Leng, Y.; Wang, J.; Zhu, D.; Shen, L.; Zhao, P.; Zhang, M. Heteropolyanion-based ionic hybrid solid: A green bulk-type catalyst for hydroxylation of benzene with hydrogen peroxide. *Chem. Eng. J.* **2011**, *173*, 620–626.
- Olivier-Bourbigou, H.; Magna, L.; Morvan, D. Ionic liquids and catalysis: Recent progress from knowledge to applications. *Appl. Catal. A: Gen.* **2010**, *373*, 1–56.
- Welton, T. Room-temperature ionic liquids: Solvents for synthesis and catalysis. *Chem. Rev.* **2011**, *111*, 3508–3576.
- Zhang, Q.; Zhang, S.; Deng, Y. Recent advances in ionic liquid catalysis. *Green Chem.* **2011**, *13*, 2619–2637.
- Deng, Y. Q.; Shi, F.; Beng, J. J.; Qiao, K. Ionic liquid as a green catalytic reaction medium for esterifications. *J. Mol. Catal. A: Chem.* **2001**, *165*, 33–36.
- Tao, D. J.; Lu, X. M.; Lu, J. F.; Huang, K.; Zhou, Z.; Wu, Y. T. Noncorrosive ionic liquids composed of [HSO₄]⁻ as esterification catalysts. *Chem. Eng. J.* **2011**, *171*, 1333–1339.
- Tao, D. J.; Wu, Y. T.; Zhou, Z.; Geng, J.; Hu, X. B.; Zhang, Z. B. Kinetics for the esterification reaction of *n*-butanol with acetic acid catalyzed by noncorrosive Brønsted acidic ionic liquids. *Ind. Eng. Chem. Res.* **2011**, *50*, 1989–1996.
- Li, K. X.; Chen, L.; Wang, H. L.; Lin, W. B.; Yan, Z. C. Heteropolyacid salts as self-separation and recyclable catalysts for transesterification of trimethylolpropane. *Appl. Catal. A: Gen.* **2011**, *392*, 233–237.
- Leng, Y.; Wang, J.; Zhu, D. R.; Ren, X. Q.; Ge, H. Q.; Shen, L. Heteropolyanion-based ionic liquids: Reaction-induced self-separation catalysts for esterification. *Angew. Chem., Int. Ed.* **2009**, *48*, 168–171.

(28) Zhao, P.; Zhang, M.; Wu, Y. Heterogeneous selective oxidation of sulfides with H_2O_2 catalyzed by ionic liquid-based polyoxometalate salts. *Ind. Eng. Chem. Res.* **2012**, *51*, 6641–6647.

(29) Leng, Y.; Zhao, P.; Zhang, M. Amino functionalized bipyridine–heteropolyacid ionic hybrid: A recyclable catalyst for solvent-free oxidation of benzyl alcohol with H_2O_2 . *J. Mol. Catal. A: Chem.* **2012**, *358*, 67–72.

(30) Zhao, P.; Leng, Y.; Wang, J. Heteropolyanion-paired cross-linked ionic copolymer: An efficient heterogeneous catalyst for hydroxylation of benzene with hydrogen peroxide. *Chem. Eng. J.* **2012**, *204*, 72–78.

(31) Leng, Y.; Ge, H.; Zhou, C. Direct hydroxylation of benzene with hydrogen peroxide over pyridine–heteropoly compounds. *Chem. Eng. J.* **2008**, *1454*, 335–339.

(32) Huang, W. L.; Zhu, W. S.; Li, H. M.; Shi, H.; Zhu, G. P.; Liu, H.; Chen, G. Y. Heteropolyanion-based ionic liquid for deep desulfurization of fuels in ionic liquids. *Ind. Eng. Chem. Res.* **2010**, *49*, 8998–9003.

(33) Tao, D. J.; Li, Z. M.; Cheng, Z.; Hu, N.; Chen, X. S. Kinetics study of the ketalization reaction of cyclohexanone with glycol using Brønsted acidic ionic liquids as catalysts. *Ind. Eng. Chem. Res.* **2012**, *51*, 16263–16269.

(34) JagadeeshBabu, P. E.; Sandesh, K.; Saidutta, M. B. Kinetics of esterification of acetic acid with methanol in the presence of ion exchange resin catalysts. *Ind. Eng. Chem. Res.* **2011**, *50*, 7155–7160.

(35) Cui, X. B.; Cai, J. L.; Zhang, Y.; Li, R.; Feng, T. Y. Kinetics of transesterification of methyl acetate and *n*-butanol catalyzed by ionic liquid. *Ind. Eng. Chem. Res.* **2011**, *50*, 11521–11527.